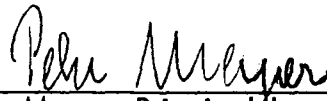


FINAL REPORT ON WORK CARRIED OUT UNDER  
GRANT NGR 14-001-196 ENTITLED  
"DEFINITION PHASE STUDY OF THE GRAND TOUR MISSIONS"



J. A. Simpson, Principal Investigator



Peter Meyer, Principal Investigator

Enrico Fermi Institute and Department of Physics  
University of Chicago

October 6, 1972

**CASE FILE  
COPY**

## TABLE OF CONTENTS

	<u>Page</u>
I. Introduction	1
II. Studies on the use of silicon detectors for low energy, low flux level measurements in the presence of RTG radiation and trapped electrons	2
RTG Radiation characteristics	4
Experimental results	6
III. High energy proton damage study of lithium-drifted and surface-barrier silicon detectors	7
IV. The gas Cerenkov counter	8
V. Studies of systems for detection of trapped high-energy protons in the presence of trapped electrons	11
VI. Reliability and redundancy studies	12
VII. List of participants in the definition of an experiment for the Grand Tour-Mariner Jupiter Saturn Missions at the University of Chicago	12
VIII. Support of Team activities by investigators	13
IX. List of accelerator runs conducted at the Space Radiation Effects Laboratory and related to the study effort	13
X. Budget	14
XI. Application of the study principles to an instrument design	14
Appendix A: Summary of High-Energy Proton Damage Study of Lithium-Drifted Detectors of December 2-5, 1971 at SREL	
Appendix B. Internal reports and memos concerning RTG interference effects and radiation damage studies.	

FINAL REPORT ON WORK CARRIED OUT UNDER  
GRANT NGR 14-001-196 ENTITLED  
"DEFINITION PHASE STUDY OF THE GRAND TOUR MISSIONS"

J. A. Simpson and Peter Meyer  
Enrico Fermi Institute and Department of Physics  
University of Chicago

October 6, 1972

I. Introduction

This is the final technical report summarizing the work carried out under NASA Grant No. 14-001-196 for the definition of an energetic particle experiment for the OPGT-MJS missions. Our proposal, dated 11 June 1971, included three studies to be carried out for the over-all development of instrumentation. These were the following:

1. The evaluation of solid state detectors and other special semi-conductor devices and their performance in the radiation environment created by RTG's and to be encountered in space by the spacecraft, including fast neutrons, protons, alpha particles, electrons, and gamma rays.

2. The investigation of an alternate system for the detection of fission fragments in the trapped proton fission detector. Specifically, the study of the construction of a pulse ion chamber which will replace the two curved solid state detectors for detecting fission currently used in the Pioneer F/G mission.

3. A study of the reliability and redundancy which may be economically achieved, and a definition of suitable means for in-flight diagnosis of component failures and the methods to provide for failure modes in which the instrumentation and sensors may be reconfigured to recover important data under circumstances where an individual component fails.

The work under this grant started out emphasizing instrumentation and detectors on the basis of an OPGT mission. Early in 1972 it became clear, however, that only the MJS scale of the mission would be viable. As a consequence some shift in emphasis in the studies under the grant was made, the most notable being the addition of Cerenkov counter studies. The EPT team in its report stressed the importance of combining the studies of galactic nuclei and electrons, but also pointed out the difficulties of achieving both within the constraints of the MJS mission as of 1972. Therefore it became part of this current objective to find out whether this was really so, or whether galactic electron instrumentation could be included and be made compatible within the scope of the MJS mission. We could show that this is indeed possible.

One further deviation from the original breakdown of the budget was made due to the difficulty of getting accelerator time for protons at the SREL facilities of NASA. This resulted in their placing hourly charges for machine time on our work. Furthermore, due to breakdowns and delays it resulted in increased travel expenses for the staff undertaking the measurements. Other than these factors the studies described follow closely the original proposal from the University of Chicago. The funds available to us for this work and for our participation in the activities of the Energetic Particles Team amounted to \$48,081. We have not fully used this amount.

II. Studies on the use of silicon detectors for low energy, low flux level measurements in the presence of RTG radiation and trapped electrons.

Of special interest in cosmic-ray studies of the interplanetary medium is the measurement of low energy (0.5 to  $\sim 2$  MeV for protons) nuclear species at low flux levels ( $10^{-3}$  to  $10^{-4}$  protons/ [cm<sup>2</sup>-sec-ster]) in the presence of background radiation from radioisotope thermoelectric generators (RTG's), and of low energy nuclei within the "trapped-radiation" regions of planets in the presence of intense electron fluxes. The

properties of the first detector of a solid state detector assembly forming a telescope for energy loss and total energy measurements are of particular concern.

Silicon detectors have been extensively used as charged-particle detectors for a number of years and a study was undertaken to determine the optimum type of silicon detector to use in the cosmic-ray studies referred to above. In general, the dimension of the sensitive area of a detector will determine the desired event rate (geometrical factor), and its sensitive "thickness" and discriminator level will determine a) lowest incident energy for analysis, b) energy range for total absorption of the particles, c) energy range for the detection of penetrating particles, for any given nuclear species. However, the "interference-level" generated in the detector by the background radiation from the RTG's via the scattering of Compton electrons, and nuclear reactions with neutrons, as well as the response of the detector to interplanetary and trapped electrons also depend on the detector area, discriminator level, and sensitive depth. An "optimized" detector for the interplanetary studies would then have the maximum area and sensitive depth, and the minimum discriminator setting consistent with a negligible RTG induced interference for a given nuclear species, with a similar situation for the case of trapped-radiation studies. Thus, measurements were needed of the basic "response" properties of the detector ("response" is defined here as the rate at which the discriminator is triggered) as a function of sensitive area, sensitive depth, discriminator level, and type of incident particle. The results of such measurements are reported here.

Before presenting a summary of the experimental results, we discuss briefly the nature of the radiation field in the vicinity of a typical RTG (extensive studies of the radiation properties of Pu O<sub>2</sub> RTG's have been reported in the literature, so that only a very brief discussion is given here).

### RTG Radiation Characteristics

RTG neutrons are generated by spontaneous fission of the plutonium, ( $\alpha, n$ ) reactions with light-element "impurities" in the fuel, and neutron multiplication. Neutrons produced by the ( $\alpha, n$ ) reaction are primarily due to alpha particles striking  $O^{17}$  and  $O^{18}$  isotopes contained in the  $Pu O_2$ . Although the natural abundance of these isotopes is quite low, their high cross section for ( $\alpha, n$ ) reactions makes them by far the largest contributors to the total neutron output. The RTG neutrons span the energy range from  $\sim 1 - 12$  MeV, with an energy spectrum which decreases strongly with increasing neutron energy. Estimates of the total neutron flux density at typical science instrument platforms for typical spacecraft RTG's are in the range  $\approx 1 - 100$  neutrons/ $[cm^2\text{-sec}]$ , depending on the "shielding" by the spacecraft and instruments, exact position of the experiment with respect to the RTG's, and "quality" of the  $Pu O_2$  fuel. Earlier studies using neutron sources showed that for neutron flux densities in this range, all silicon detectors used at LASR would have a negligible response to RTG neutrons for all detector sensitive depths used in LASR experiments. Details of these measurements are not presented here.

Most of the gamma radiation from the RTG fuel comes from the gamma emitting impurities contained in the fuel and from gamma emission which accompanies alpha decay of  $Pu^{238}$ . As discussed in the EPT report of 30 April 1972, the gamma flux and spectrum from plutonium-238 changes significantly with the fuel age. For fuel ages less than one year, the predominant source is gamma emission which accompanies alpha decay of  $Pu^{238}$ . However, spontaneous fission, fission products, ( $\alpha, n$ ) reactions, and other sources are also contributing factors. For older fuel, plutonium -236, which is an impurity present in trace quantities in the fuel, becomes the main contributor of gamma emission. The  $Pu^{236}$  decay chain produces a large number of daughter nuclides

which emit gamma radiation. The  $Tl^{208}$  which results from the decay of the  $Pu^{236}$  gives rise to a 2.614 MeV gamma, which increases in intensity with time. Essentially all of the  $\gamma$ -rays emitted by the RTG's span the energy range from 17 KeV to 2.6 MeV. A few high energy fission gammas (up to 7 MeV) are present, but are extremely "faint". However, although there are numerous gammas with energies below  $\sim 700$  keV, most of them are attenuated due to self absorption in the fuel, the capsule walls, and the outer RTG structure so that only a small fraction escapes. Thus, at a point at some distance from the RTG's, most of the gammas are concentrated at energies near  $\sim 800$  keV and 2.6 MeV. For example, at the position of the University of Chicago experiment on the Pioneer F/G spacecraft, the total flux density is  $\sim 130$  photons/ (cm<sup>2</sup>-sec), with 60% of the gammas at  $\sim 800$  keV and 30% at 2.6 MeV. Estimates of the total gamma flux density at the science scan platform on MJS range from 34 to 226 photons/ (cm<sup>2</sup>-sec), depending on the spacecraft attenuation assumed, so that the gamma flux density for the MJS experiment is comparable to that for the Pioneer F/G.

From the above, it is clear that it would be virtually impossible to accurately simulate the actual gamma spectrum and flux density which would exist at any point on, for example, the MJS (or any other) spacecraft. However, earlier studies on a thin (34  $\mu$ ) detector showed that the response of the detector to  $Na^{24}$  gammas (2.76 MeV) was comparable to the response of the detector to  $Co^{60}$  gammas (1.17 and 1.33 MeV). Also, the  $Co^{60}$  gammas are fairly close in energy to the majority of RTG gammas. Therefore, response studies making use of  $Co^{60}$  should permit reliable predictions as to the response expected for actual RTG's.

### Experimental Results

To establish the response of silicon detectors of different sensitive depths to  $\text{Co}^{60}$  gammas and electrons of various energies, "calibrated"  $\text{Co}^{60}$  and electron sources ( $\text{Bi}^{207}$ ,  $\text{Sr}^{90}$ ,  $\text{Cs}^{137}$ ) were used with detectors with sensitive depths from  $35.7 \mu$  to  $125 \mu$ . The output signals from the detectors were pulse-height analyzed using standard electronics. The results of the measurements are given in Table 1, where the strong dependence of detector response on detector sensitive thickness and discriminator level is clearly evident. To show the strong dependence of response on detector sensitive depth more clearly, Fig. 1 is a plot of the entries in Table 1 for  $\text{Co}^{60}$   $\gamma$ -rays and a discriminator setting of 350 keV. Over the range of detector depths studies, the response (counts/sec  $\geq$  given discriminator level) for a 350 keV discriminator level and  $\text{Co}^{60}$   $\gamma$ -rays varies as  $W^x$ , where  $W$  is the sensitive depth and  $x \sim 5.4$ . Fig. 2 is a plot of the entries in Table 1 for  $\text{Sr}^{90}$  electrons and a discriminator level of 350 keV. The dependence of response on  $W$  shown in Fig. 2 is again very strong, the variation being  $\sim W^y$ , where  $y \sim 6.4$ .

The data given in Table 1 provide the information necessary to estimate the response of a detector with sensitive depth in the range  $35 - 125 \mu$  to RTG  $\gamma$ -rays for a range of discriminator settings. For example, on the basis of these investigations we find that for a  $1 \text{ cm}^2$  detector with a sensitive depth of 70 microns and a discriminator set at 400 keV, we can measure proton intensities above  $\sim 0.1$  protons/ $(\text{cm}^2\text{-sec})$  at energies as low as  $\sim 0.4$  MeV, all in the presence of  $\sim 1 - 2$  MeV electron fluxes as high as  $\sim 10^3 / \text{cm}^2\text{-sec}$ . Also, for the same detector, we can measure proton intensities above  $\sim 0.3$  protons/ $[\text{cm}^2\text{-sec}]$  at energies above  $\sim 0.4$  MeV in the presence of 1 MeV  $\gamma$ -ray fluxes as high as  $\sim 3 \times 10^5$  gammas/ $[\text{cm}^2\text{-sec}]$ . For the interplanetary

studies proposed for the MJS, this is equivalent to permitting the RTG gamma intensity to grow by a factor of  $\sim 10$  over a period of  $\sim 6$  years without obscuring the measurements of these low flux ( $10^{-3} - 10^{-4}$  protons/[cm<sup>2</sup>-sec-ster]) low energy ( $\sim 0.5 - 2$  MeV protons) nuclei. Very recently, this was borne out by our preliminary results from the detector assembly on Pioneer 10 which is very similar to that proposed for the MJS where we have found that the maximum interference level from the Pioneer 10 RTG radiation will be an order of magnitude below any expected primary flux even taking into account the growth of the RTG gamma ray background during the life of the mission.

In summary, we find that for the MJS mission, a suitable detector for the first detector of a telescope fulfilling all the demands for background protection against electrons and RTG radiation, for adequate lifetime, and for sufficient response to make energy loss measurements for all nuclei, can have the following characteristics: a) sensitive depth = 70 microns; b) sensitive area =  $2.5 \text{ cm}^2$ ; c) operating bias = 30 volts.

### III. High energy proton damage study of lithium-drifted and surface-barrier silicon detectors.

For any silicon detector which is to be exposed to proton fluxes over an extended period of time, the problem of resulting "radiation damage" is of concern. This is particularly true for lithium-drifted detectors which, in general, are operated at lower electric field intensities than conventional surface-barrier detectors. To establish the integrated proton flux levels at which damage is apparent for lithium-drifted and surface-barrier detectors of the type fabricated at our laboratory, a number of detectors were irradiated with high-energy protons at the SREL. A report summarizing the results of this study for the lithium-drifted detectors is given in Appendix A. Summarizing the

overall results briefly, four lithium-drifted silicon detectors with sensitive depths ranging from  $\sim 500$  microns to  $\sim 1500$  microns and operated from 20 to 40 volts bias were irradiated with protons of energy 200 MeV, 300 MeV, and protons covering the energy range from  $\sim 50 - 570$  MeV, to a level of  $\sim 3 \times 10^8$  protons/cm<sup>2</sup>. All detectors showed an increase in leakage current of about a factor of two. The detectors with sensitive depths less than  $\sim 1000$  microns showed no degradation in their response to low-energy  $\alpha$ -particles and electrons, whereas the detectors with sensitive depths greater than 1000 microns showed a marked decrease ( $\sim 20\%$ ) in their charge-collection efficiency for low-energy (5.48 MeV)  $\alpha$ -particles and a degradation in resolution. For the surface-barrier type fission fragment detectors, the response of two curved surface-barrier detectors to Cf<sup>252</sup> fission fragments was measured before and after exposure of the detectors to  $4.5 \times 10^8$  protons/cm<sup>2</sup> in the energy range 51 to 570 MeV. Their fission fragment response showed no measurable change following proton exposure.

Additional internal reports concerned with RTG interference studies and radiation damage are listed in Appendix B.

#### IV. The gas Cerenkov counter

The EP report (April 30, 1972) stresses the importance of simultaneous measurements of nuclear and electron energy spectra on MJS: "High energy electron spectra are crucial in the establishment of a quantitative basis of the theory of non-thermal radio emission from planetary objects and the galaxy. Since the non-thermal galactic radio emission in effect is believed to be largely a spatial integral of synchrotron radiation, local measurements of the interstellar electron spectrum would allow deductions on the general distribution of cosmic rays in the galaxy. Also, due to a charge to mass ratio drastically different from that of nuclei, electron data provide important clues to the study of the solar modulation of galactic cosmic rays, and their heliocentric intensity gradient may differ substantially from that of nuclei." At the

same time the EP report emphasizes the difficulty of accommodating an electron experiment within the MJS mission concept. As noted above, we included the investigation of this question as part of the present study, the prime factors being weight, power and cost required for a gas-Cerenkov counter needed for the electron experiment. Further, the gas Cerenkov counter had to be miniaturized to a size compatible with the present practical limits of a solid state detector telescope.

A gas Cerenkov counter was first used in a satellite experiment by this laboratory on OGO-5 for a cosmic ray electron experiment. Its purpose was to provide discrimination between relativistic electrons and the intense background of low energy protons, and to use the directional discrimination necessary to eliminate spurious events resulting from backward moving particles.

A model of a gas counter which fulfills the requirements for an MJS mission was developed and tested during the study period under this grant. The counter must have high efficiency of response to electrons, be immune to low energy protons (i. e., the gas must not emit scintillation light), and be sufficiently small. The gas used as a Cerenkov radiator must have a high inherent refractive index to minimize the operating pressure, but must not liquify at the required pressure and the lowest operating temperatures to be encountered by the equipment. In addition, the gas must be transparent to a major portion of the spectrum emitted in Cerenkov radiation.

A series of tests were performed at the SREL Cyclotron and with mu-mesons. These demonstrated that ethylene gas at a pressure of 17.5 atmospheres (at 0°C) fulfilled all of the above conditions. It provides a threshold of 2.5 MeV for electrons and 5 GeV for protons. Further testing with other gases, as well as ethylene, demonstrated the absence of any measurable scintillation in the ethylene. The

performance of the model counter in a run with cosmic ray muons is illustrated in Figure 3. The data show the pulse height distribution with a Cerenkov counter having blackened walls. The distribution is consistent with calculations.

Tests to determine the scintillation of various Cerenkov counter gases were performed by exposing the system to a beam of 195 MeV protons at SREL. Results of these runs with neon,  $SF_6$  and ethylene are shown in Figure 4 for a counter in which the walls were coated with a diffuse high reflectance material. The threshold of the photomultiplier was set to one photoelectron, which is the "signal" referred to in Fig. 4. This figure illustrates the relative response of the three gases being investigated, and the absence of scintillation light from ethylene.

Since ethylene -- in contrast to  $SF_6$  -- also has excellent thermal properties (It will liquify only at  $-40^{\circ}C$ , if the pressure is 18 atmospheres at  $0^{\circ}C$ ), it is the suitable gas for this counter.

Therefore it is a conclusion of our study that galactic nuclei and electrons can simultaneously be studied in one instrument which falls well below the limits of the specifications for charged particle experiments on the MJS mission. The miniaturized gas Cerenkov counter can be inserted in a solid state detector particle telescope.

Earlier tests of the OGO-5 gas Cerenkov counter exposed to the Pioneer F/G RTG's have shown that the induced background counting rate is far below the level that would cause interference with the performance of the detector. Applying these results to the model gas Cerenkov counter for MJS does not alter these conclusions.

V. Studies of systems for detection of trapped high-energy protons in the presence of trapped electrons.

Because of the exceedingly high intensity of trapped electrons in the Jovian radiation belt a new concept was developed for the detection of high energy protons. This concept was to provide immunity from electrons through employing proton induced fission where the fission fragments releasing  $\sim 50$  to  $90$  MeV energy in a detector would under no circumstances be confused with electron pile-up. This concept was implemented in Pioneer-10 as shown in Figure 5, where the fissionable material chosen was  $\text{Th}^{232}$  and where the fission fragment detectors were silicon surface-barrier detectors. Such a system requires a basic volume for each foil element of magnitude shown in Figure 5. Therefore, in order to extend these principles for future investigations we have noted that the detection of fission fragments in a pulse ion chamber has many attractive features. The number of foils of fissionable material can be substantially increased within a small volume so as to reduce the lower limit of proton flux detection in passing through the Jovian belt by at least an order of magnitude for protons above  $30$  MeV/nucleon, and to further reduce the contribution of direct background counts from possible trapped carbon, oxygen and higher Z nuclei in the Jovian belt. In this concept a series of alternating ion collection plates and fission foils can be "stacked" with a very small plate spacing. It was part of the purpose of this grant to build a bench test prototype of this concept. The prototype system now in operation is shown in cross-section in Figure 6. The gas used is 95% Argon and 5% carbon dioxide, and is operated at 18 atmospheres pressure. The chamber is presently operating with a plate spacing of  $0.62$  mm. It is currently under test with alpha particles and

will soon undergo additional tests with fission fragments using high intensity neutron sources. On the basis of calculation, we predict that high intensity trapped electrons will not interfere with fission fragment measurements above say 50 MeV energy. We are continuing the evaluation of this model and plan studies with high intensity electron sources and cyclotron runs with alpha particles and protons. The cyclotron runs are planned for late November 1972 at SREL. Additional work will be carried out using other funds.

#### VI. Reliability and redundancy studies

As a result of the increased emphasis on the MJS type instrumentation the study touched only slightly on the subject of reliability and redundancy, with the exception of how electron and nucleon experiments, carried out in combination, could adapt to failure modes and to reconfigurations of sensor assemblies to insure recovery of data on a long term flight.

Additional items investigated which we wish to mention are:

1. Gain shifts in photomultiplier tubes as a result of exposure to the Jovian radiation environment. A system of commandable photomultiplier voltage levels was studied.
2. Command schemes have been investigated which would enable reconfiguration of detector amplifiers and discriminators if one, critical to the operation of the system, should fail.

#### VII. List of participants in the definition of an experiment for the Grand Tour-Mariner Jupiter Saturn Missions, at the University of Chicago.

In addition to the Principal Investigators, the following LASR personnel have participated in the study efforts supported by this grant:

Dr. M. Garcia Munoz	Mr. D. Hunsinger
Dr. G. M. Mason	Mr. G. Lentz
Dr. B. G. Cartwright	M. H. Thomas
Dr. P. Evenson	Mr. M. Weber
Dr. A. Tuzzolino	Dr. A. Mogro-Campero
Mr. J. E. Lamport	Mr. D. Hamilton
Mr. M. Perkins	Mr. S. Tejero
Mr. R. Jacquet	

VIII. Support of Team activities by investigators

The principal investigators are members of the EP team. Their participation in the following meetings was covered under this grant.

April 30, 1971	Meyer, Simpson	Washington
May 10-11, 1971	Meyer	Pasadena
June 14-15, 1971	Meyer, Simpson	Pasadena
Dec. 17-18, 1971	Meyer, Simpson	Chicago
Apr. 29, 1972	Simpson	Washington

IX. List of accelerator runs conducted at the Space Radiation Effects Laboratory and related to the study effort.

October 9, 1971, tests of solid state fission systems.

December 1, 1971, tests of solid state fission system and radiation damage effects from protons.

May 18, 1972, tests of solid state fission systems and gas Cerenkov system.

July 30, 1972, tests of fission system and instrument response to re-configuration commands.

X. Budget

Grant NGR 14-001-196 was funded in the amount of \$48,081. A breakdown of the expenditures for the definition effort detailed above is shown below.

Total Award	\$48,081
<u>Estimated Expenditures to 9-30-72</u>	
Salaries	\$ 20.0 K
Employee Benefits	2.2
Indirect Cost	10.4
Supplies and Services	5.5
Travel	3.7
Computer Services	<u>0.2</u>
Total Estimated Exp.	<u>\$ 42.0 K</u>
<u>Estimated Unexpended Funds</u>	
<u>on 9-30-72</u>	<u>\$ 6.1 K</u>

XI. Application of the study principles to an instrument design

Using other funds, the concepts arrived at in this definition phase study for an energetic particle experiment on an OPGT/MJS mission have subsequently been used in the design of a prototype instrument which will reach the most important scientific goals defined in the report of the EP team (document dated April 30, 1972). In particular it was possible to arrive at a single instrument in which the measurement of nuclei, charge composition, isotopic composition and electrons over a wide energy range can be accomplished, a goal specifically stated in the EPT report. The design

specifications conservatively meet the constraints in weight, power and size, imposed by the MJS mission. In Fig. 7 we show a schematic cross-section of this prototype instrument, and in Table 2 we present a list of the types of particles that can be observed and the range of energies over which their spectra can be determined by this instrument.

## Appendix A

### Summary of High-Energy Proton Damage Study of Lithium-Drifted Detectors of December 2-5, 1971 at SREL

Tony Tuzzolino

A Pioneer F/G type fission system was "calibrated" and high-energy proton damage of Lithium-drifted detectors was studied during the period December 2-5, 1971, at the SREL. LASR personnel at the site were A. Tuzzolino, D. Hamilton, and F. Sopron. Most of the "beam time" was devoted to the Fission system so that only a limited amount of proton-damage data was obtained. The results obtained for the proton damage study are given below:

#### High Energy Proton Damage to Lithium-Drifted Silicon Detectors

Unfortunately, an insufficient amount of time was available for the radiation damage studies intended. However, some limited data was obtained on four detectors. Their characteristics and exposure received are as follows (w = sensitive depth in microns; T = total detector thickness in microns; V = operating bias in volts; A = area of the sensitive surface in  $\text{cm}^2$ ; E = total exposure in protons/ $\text{cm}^2$  of a given energy):

Detector No. 1: L - 1333 (flat); W = 506; T = 551; V = 20; A = 6.6; E =  $3.7 \times 10^8$  protons/ $\text{cm}^2$  of energy 300 MeV.

Detector No. 2: L - 1153 (flat); W = 1029; T = 1118; V = 20; A = 9.1; E =  $2.7 \times 10^8$  protons/ $\text{cm}^2$  of energy 300 MeV.

Detector No. 3: L - 1152 (flat); W = 1448; T = 1549; V = 40; A = 9.1; E =  $1.2 \times 10^8$  protons/ $\text{cm}^2$  of energy 200 MeV.

Detector No. 4: L - 1335 (curved); W = 1405; T = 1515; V = 40;

A = 9.1; total exposure as follows:

proton energy (MeV)	E (protons/cm <sup>2</sup> )
51	$2.2 \times 10^7$
79	$3.9 \times 10^7$
143	$3.5 \times 10^7$
175	$4.5 \times 10^7$
278	$2.7 \times 10^7$
386	$5.2 \times 10^7$
480	$3.3 \times 10^7$
570	$5.1 \times 10^7$

or a total E of  $3.1 \times 10^8$  protons/cm<sup>2</sup> distributed over the indicated proton energies.

The detectors were characterized both before and after the exposure by measuring a) leakage current; b) electrical "noise"; c) charge-collection-efficiency and particle resolution for Am<sup>241</sup> ( $\alpha$  particles of 5.48 MeV) and Bi<sup>207</sup> (electrons) sources.

Since questions relating to levels of acceptable damage and the mechanisms involved have been brought up a number of times in the past, a brief discussion of those aspects of radiation damage which are related to such questions will be given first to demonstrate, in fact, that a unique, quantitative answer to any given question can, in general, not be given.

Aside from considerations of the long term "noise-stability" of the lithium-drifted silicon surface-barrier detector, the ultimate usefulness of lithium-drifted silicon detectors in space applications will be determined by their sensitivity to radiation damage. Up to the present time, limited experimental information is available concerning the effects of radiation damage on the characteristics of lithium-drifted silicon detectors. Unfortu-

nately, there is considerable uncertainty in the application of calculated rates of defect production to accurate predictions of the effects of actual damage on the charge-collection-efficiency, energy resolution, leakage current, electrical noise, and carrier transit times of such detectors. In any case, the following will attempt to 1) describe in a qualitative manner, the mechanisms involved in radiation damage, 2) indicate the "amount" of damage to be expected from a few representative particles of given energies.

From the point of view of the use of silicon detectors as charged particle spectrometers, the only useful interactions between radiation and the detector material are those producing electron-hole pairs in the material. In this case, the normal equilibrium of the material is restored in a very short time and we use only the transient effect for measurements. However, radiation in its many forms can interact with atoms in the lattice structure and displace them from their lattice sites. Each such interaction produces at least one vacancy and an interstitial atom in the lattice (Frenkel defect). In general, the atom ejected from its lattice site carries enough energy to displace further atoms, and more than one vacancy--interstitial (defect) pair is produced. The number of defects produced by a single interaction and the probability of occurrence of a damaging interaction depends upon the type and energy of the radiation. This problem has been treated a number of times in the literature and some of the results given in these treatments will be used here. The electrical behavior of the semiconducting material (silicon) used in detectors is governed by very small impurity concentrations. Since the centers created by irradiation may be just as "active" as the original impurity concentrations, semiconductor materials (in particular silicon) are very sensitive to radiation damage.

The problem of radiation damage in semiconductors is usually divided into two parts. The first and simpler problem is the spatial distribution and density of defect centers. The second and far more complicated one concerns

the effects of these centers on the electrical and detection characteristics of the device. Interactions between defects and between defects and impurity centers makes an analysis of the overall effect quite complex. However, it has been possible to estimate the number of defects introduced in a number of different cases.

We consider collisions between an incoming particle and the semiconductor atoms. Gamma rays interact in the material to produce free electrons with energies ranging up to the gamma ray energy and, therefore, the damage they produce is similar to that produced by incident fast electrons. Different types of particles react with the lattice in different ways and this causes the amount and character of the damage to differ considerably. Fast neutrons have very low probability of producing direct "hits" with silicon atoms but the average energy acquired by the silicon atoms from the collisions is quite high. The resulting energetic silicon atom produces many secondary defects and the overall damage is characterized by small highly damaged regions separated by considerable amounts of undamaged material.

On the other hand, heavy charged particles interact with silicon atoms by Rutherford scattering so that there are large numbers of low energy exchanges and very few silicon atoms acquired high enough energies to produce substantial numbers of secondary defects. Damage by fast electrons is influenced largely by the fact that a silicon atom can acquire little energy when an electron collides with it. Therefore, damage is limited almost entirely to the few silicon atoms which acquire sufficient energy to be displaced from the lattice. For low electron energies ( $< 250$  KeV in silicon), no collision can give sufficient energy to a lattice atom to displace it. Measurements of the energy ( $E_d$ ) required to displace a silicon atom indicate that 25 to 30 eV is necessary.

Even for electrons having energies up to 10 MeV, the energy transferred to recoiling ions is low so that complex localized regions of damage which result from a cascade of displacements are avoided and, in contrast with the case of fast neutron damage, electrons produce a relatively uniform distribution of defects.

The case of slow neutron damage is somewhat different from those discussed above. Here, the capture of a neutron by  $\text{Si}^{30}$  (4% of silicon) produces  $\text{P}^{31}$  and a  $\beta$ -particle whose energy ranges up to 1.5 MeV. Damage of the vacancy-interstitial type is produced by the electrons as in the previous paragraph. However, the phosphorus atom now acts as a donor in the lattice and the bulk resistivity changes. This can be considered as damage or a desirable effect depending upon its effect on detector performance. Fortunately, the cross section for this process is small.

The intense damage spike produced by the entry of highly charged particles (fission fragments) is too complicated a process to permit detailed understanding and will not be discussed here.

From these brief considerations, we conclude that the most important types of damage result from fairly heavy charged particles (such as protons and  $\alpha$ -particles) and from fast neutrons and electrons.

In the case of charged particles such as  $\alpha$ -particles, the mean energy acquired by the primary silicon recoils is low but the number of primary recoils is large.

Figure 1 is a calculated curve giving the number of defects produced as a function of proton energy, and Figure 2 is a calculated curve giving the number of defects per cm as a function of the energy of protons and alphas.

Integration of the curve shown in Figure 2 to determine the total number of defects produced by a 40 MeV  $\alpha$ -particle shows that it leaves about 400 defects along its track (range in silicon of  $\sim 800 \mu$ ). This means that an integrated flux of  $10^8$  alphas/cm<sup>2</sup> (40 MeV) will give rise to a defect density of  $\sim 5 \times 10^{11}$  defects/cm<sup>3</sup> in a piece of silicon  $800 \mu$  thick. A similar integration of the proton curve shown in Figure 2 shows that an integrated flux of  $5 \times 10^8$  protons/cm<sup>2</sup> at an energy of 10 MeV will give rise to this same defect density in a  $800 \mu$  thick piece of silicon. For fast electrons (see Figure 3), approximately  $10^{11}$  electrons/cm<sup>2</sup> would be required.

It should be noted that the defect density is very high at the end of range of the damaging particle (Fig. 2). Thus for damaging particles having a range less than the sensitive depth of the detector, the "extent of the damage" or defect density is a strong function of position in the sensitive region of the detector and consequently, those "material" characteristics which determine the charge-collection-efficiency and particle "resolution" (carrier recombination lifetime; "plasma" time; trapping lifetime; local electric field intensity) will also depend strongly on position. An additional complication may be the particular choice of amplifier shaping time constant, although this aspect will not be discussed here.

From the above, it turns out that bulk damage in lithium-drifted detectors will affect the detector performance in two ways. The first (and probably most important) effect of the damage will be to prevent total depletion of the original sensitive depth by the applied bias. This will lead to poor (if not negligible) charge collection over a portion of the original sensitive depth. The second effect of the damage will be to introduce levels in the forbidden gap of silicon which may act as recombination and trapping centers. Consequently, the detector leakage current will tend to increase and the degradation (produced by the damage) in the carrier lifetimes and mobilities (and consequently, the carrier transit times) may cause a

significant loss of charge during the charge collection process even in regions where the field has not been affected significantly by the damage. This second effect is too complex to treat quantitatively and will not be considered here. As an indication of the particle flux levels at which the first effect of damage (incomplete depletion of the original intrinsic depth) may begin to be observed, we consider the case of a lithium-drifted detector with an original intrinsic depth  $W_0$  of  $800\mu$  operated at a bias  $V_0$  of 50 volts. If the detector has been carefully drifted, the lithium ion concentration (donor impurity) will be such as to very accurately "compensate" the concentration of initial acceptors. Application of a bias  $V_0$  will give rise to a uniform electric field  $E_0$  throughout the intrinsic region. If, following radiation damage, the applied bias  $V_0$  is still to deplete the entire depth  $W_0$ , then calculation shows that the defect concentration (assuming uniform defect concentration throughout  $W_0$  and that each defect behaves as an acceptor) must be less than  $\sim 1.5 \times 10^{11}$  defects/cm<sup>3</sup>. If we consider, first, damage by low energy particles, calculations using Figures 1 through 3, show that this defect concentration will be produced by integrated fluxes of approximately  $3 \times 10^7$  alpha particles/cm<sup>2</sup> (40 MeV),  $1.5 \times 10^8$  protons/cm<sup>2</sup>, and  $3 \times 10^{10}$  fast electrons/cm<sup>2</sup>. Although these calculations are highly qualitative, those limited experimental studies which have been carried out on damage in lithium drifted silicon detectors by low energy protons and  $\alpha$ -particles show, in fact, that the effects of damage become evident at just about these doses.

These studies also show that for a given detector damaged by given particles of given energy, it's response to different particles spanning a range of incident energies may vary from completely undegraded response, to severely degraded response. Also, the operating bias chosen for the detector is of extreme importance in determining the observable effects of the damage. For example, if an undamaged detector is operated at a bias voltage just barely sufficient to satisfy the "requirements" of "good" charge collection and adequate transit time for carriers, then after being damaged,

it's response will be poorest at this operating bias versus higher biases, and it's response will improve monotonically with increasing operating bias voltages.

For particles of fairly high energy ( $\approx 100$  MeV and greater), the defect density should be fairly uniform, which would then somewhat simplify any analysis of the observable effects of the damage. In summary, it is, in general, not possible to answer specific questions related to the performance expected from a lithium-drifted or conventional surface-barrier detector following a given exposure to particles in a quantitative manner. For a given exposure to a damaging particle, the degree to which the response of a detector to this same particle, or to particles other than those responsible for the damage, will be degraded can be determined only by direct measurement. In addition, the integrated flux levels which may be tolerated for a given detector will depend strongly on a) the overall requirements of the experiment (requirement on charge-collection-efficiency, electrical resolution, charged-particle resolution, leakage current, etc.), b) the temperatures to which the detector will be exposed in the experiment (which will determine the maximum allowable electric field), c) the various "time-constants" permissible for the amplifiers and the discriminator levels.

#### Experimental Results of Proton Damage

Detector No. 1: From the sensitive depth and applied bias we have that the bulk electric field is  $\sim 400$  v/cm and the maximum carrier transit time is  $\sim 0.25\mu$  sec. All detector characteristics were unaffected by exposure to  $3.7 \times 10^8$  protons/cm<sup>2</sup> (300 MeV), except that the leakage current increased by  $\sim$  factor of 2.

Detector No. 2: The bulk electric field for this detector is  $\sim 200$  v/cm and the maximum carrier transit time is  $\sim 1.0\mu$  sec. At the operating bias of 20V, the charge-collection efficiency and particle resolution

for  $\alpha$ -particles was "barely" acceptable. In spite of this, all detector characteristics were unaffected by exposure to  $2.7 \times 10^8$  protons/cm<sup>2</sup> (300 MeV), except that the leakage current increased by  $\sim$  factor of 2.

Detector No. 3: The bulk electric field is  $\sim 275$  v/cm and the maximum carrier transit time is  $\sim 1.0\mu$  sec. For this detector, there was a measurable degradation in all of its characteristics. Fig. 4 shows the response to Am<sup>241</sup>  $\alpha$ -particles (5.48 MeV) before exposure to protons. Here is also a case where, at 40V bias, the charge-collection-efficiency for  $\alpha$ 's is just barely acceptable (95%). Fig. 5 shows the response of the detector to Bi<sup>207</sup> electrons, also before exposure to protons. The leakage current is  $\sim 2.5\mu$  amp., the electrical resolution is 50 KeV (FWHM), and the detector has acceptable response to the conversion electrons from Bi<sup>207</sup> (0.482, 0.554, 0.972, and 1.044 MeV). The resolution of the 0.972 MeV conversion electron line is 71 KeV (FWHM), and the 0.482 and 0.554 conversion electrons are clearly resolved. Also, the 0.972 and 1.044 MeV conversion electrons are almost resolved. Fig. 6 shows the response of the detector to Am<sup>241</sup>  $\alpha$ 's after an exposure of  $1.2 \times 10^8$  protons/cm<sup>2</sup> of 200 MeV energy. One sees that the charge-collection efficiency has degraded from 95% (Fig. 4) to 75% and the  $\alpha$  resolution has degraded considerably. The leakage current after exposure ( $\sim 7\mu$  amp) is  $\sim$  a factor of 2 greater than before exposure ( $\sim 2.5\mu$  amp), so that it's electrical resolution is somewhat degraded. Fig. 7 shows that when the applied bias is increased to 80 volts, the response to  $\alpha$ 's after proton exposure is approximately the same as the response of the detector to  $\alpha$ 's at 40 volts bias before proton exposure, so than an increase in bias  $\sim$  a factor of two is required to restore the  $\alpha$ -response to its initial value at the initial bias. Fig. 8 shows the response to Bi<sup>207</sup> after proton exposure and one sees that the response to electrons is also degraded. The 0.482 and 0.554 MeV conversion

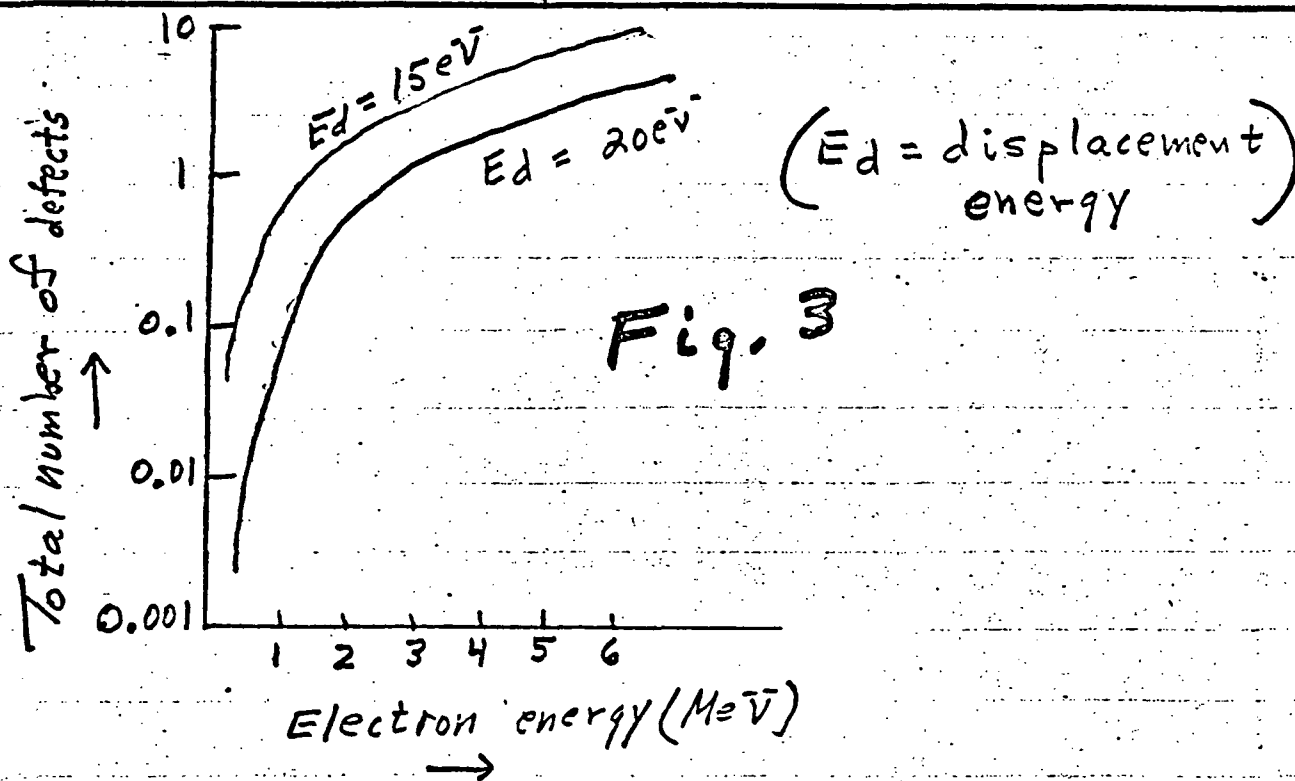
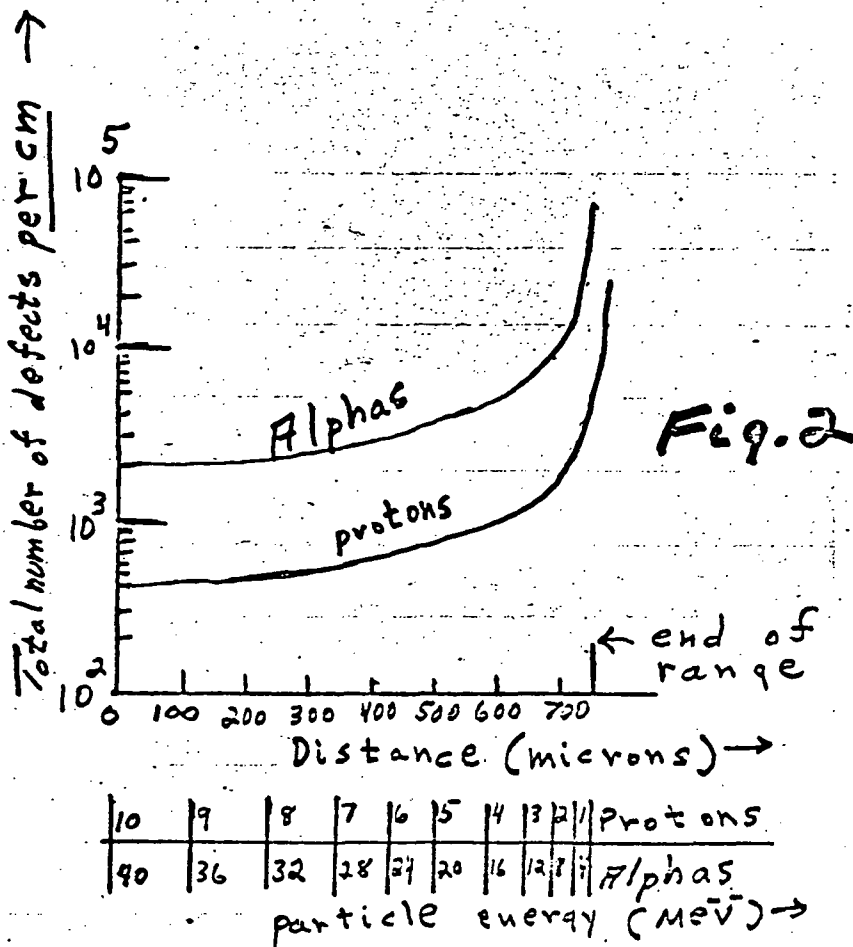
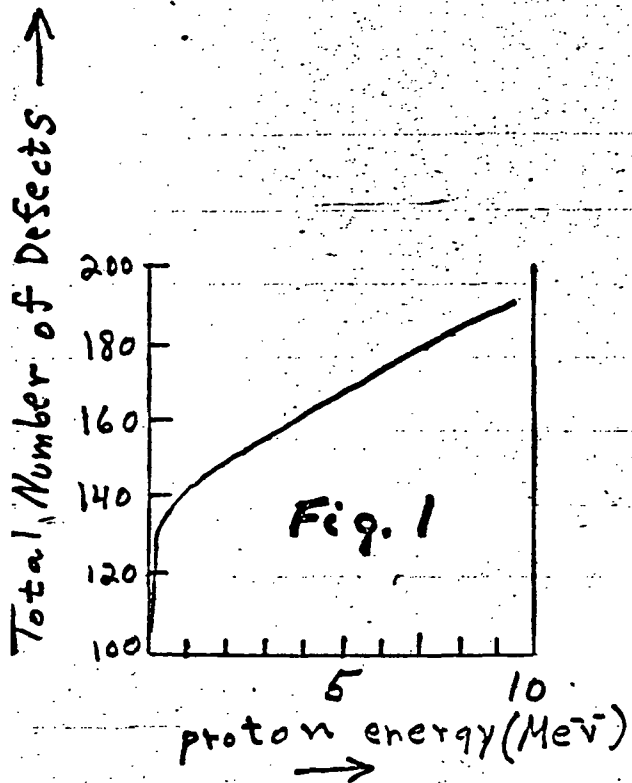
electrons are no longer clearly resolved, there is no longer any evidence of any separation between the 0.972 and 1.044 MeV conversion electrons, and the electrical and 0.972 MeV conversion electron resolutions are degraded.

Detector No. 4: The bulk electric field is  $\sim 286$  v/cm and the maximum carrier transit time is  $\sim 1.0\mu$  sec. As with detectors No. 2 and 3, the charge-collection-efficiency before proton exposure was barely acceptable at the operating bias and detector No. 4 showed a degraded response to both  $\alpha$  particles and electrons following an exposure of  $3.1 \times 10^8$  protons/cm<sup>2</sup> distributed in energy from  $\sim 50$  to 600 MeV. The degradation in  $\alpha$  and electron response was comparable to the degradation observed for detector No. 3. The leakage current for detector No. 4 had also increased by  $\sim$  factor of 2.

### Conclusion

Of the four lithium-drifted detectors exposed to high-energy protons, two of them showed measurable degradation in their response to low-energy  $\alpha$ -particles and electrons, in spite of the fact that their nominal bulk electric fields and carrier transit times were comparable to those which showed no degradation. All four detectors showed an increase in leakage current  $\approx$  a factor of 2 after proton exposure.

No attempt is made here to relate the observed degradation to specific damage mechanisms discussed earlier. The results of this study show that lithium-drifted detectors exhibit differing degrees of degradation in their response to  $\alpha$ -particles and electrons following exposure to high-energy protons to a level of  $\sim 3 \times 10^8$  protons/cm<sup>2</sup>.



Calculated Curves

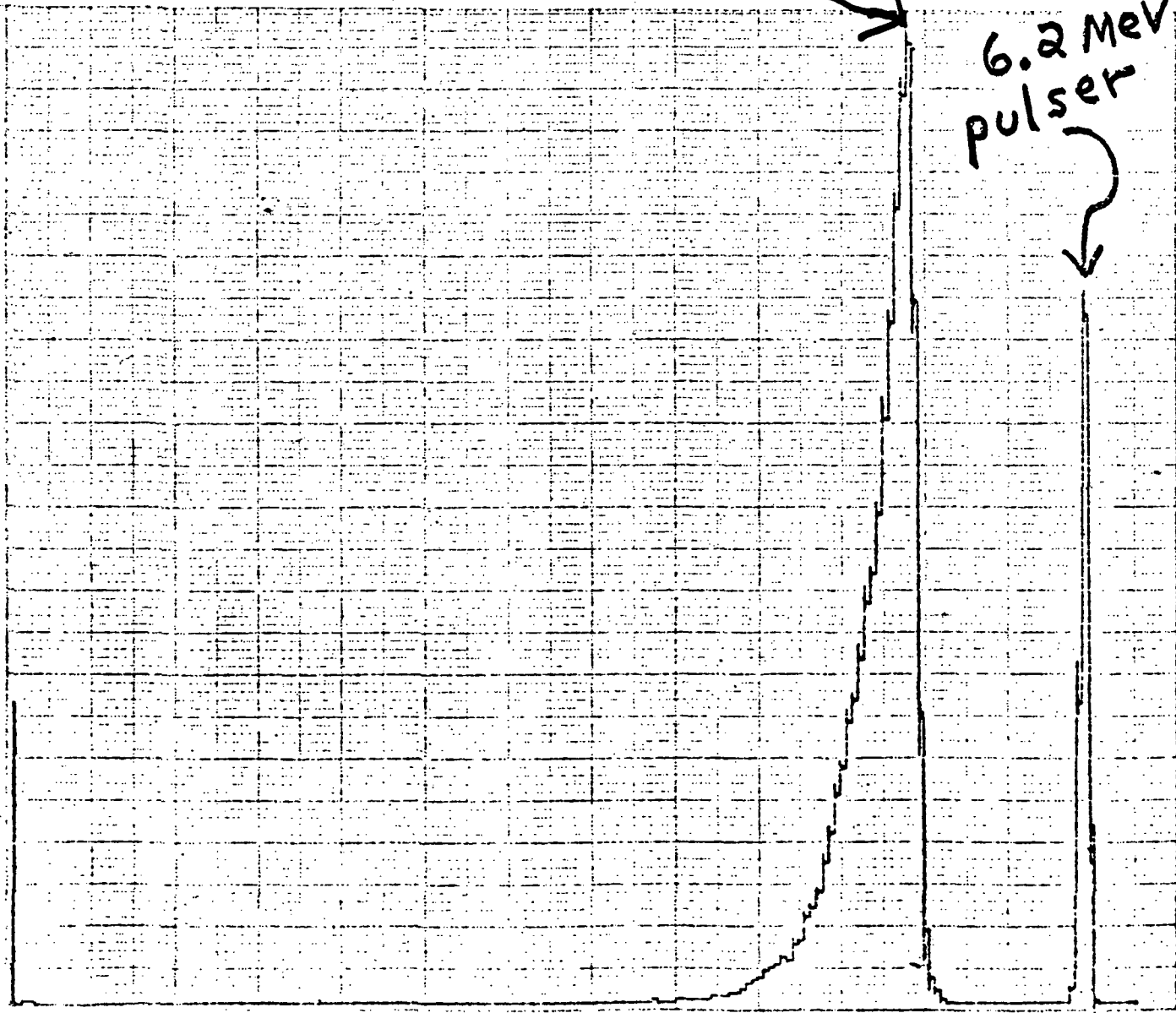
Det. #	L-1152	
Date:	11/29/71	Time
Run #		Spec. #
Volts	40 Volts   2.5 $\mu$ A	
Press.	F. Pump	Temp. Room $^{\circ}$ C
Pulser	6.2 MeV	Source Am <sup>241</sup>
$\Delta t$	1.0'	Amp. Const. 1 $\mu$ S
F.W.H.M.		C.C.E.
Stored in		Horz. Scale

Am <sup>241</sup> spectrum taken  
Before exposure to  
protons

Figure 4.

Am <sup>241</sup>  
(5.22 MeV)

6.2 MeV  
pulser

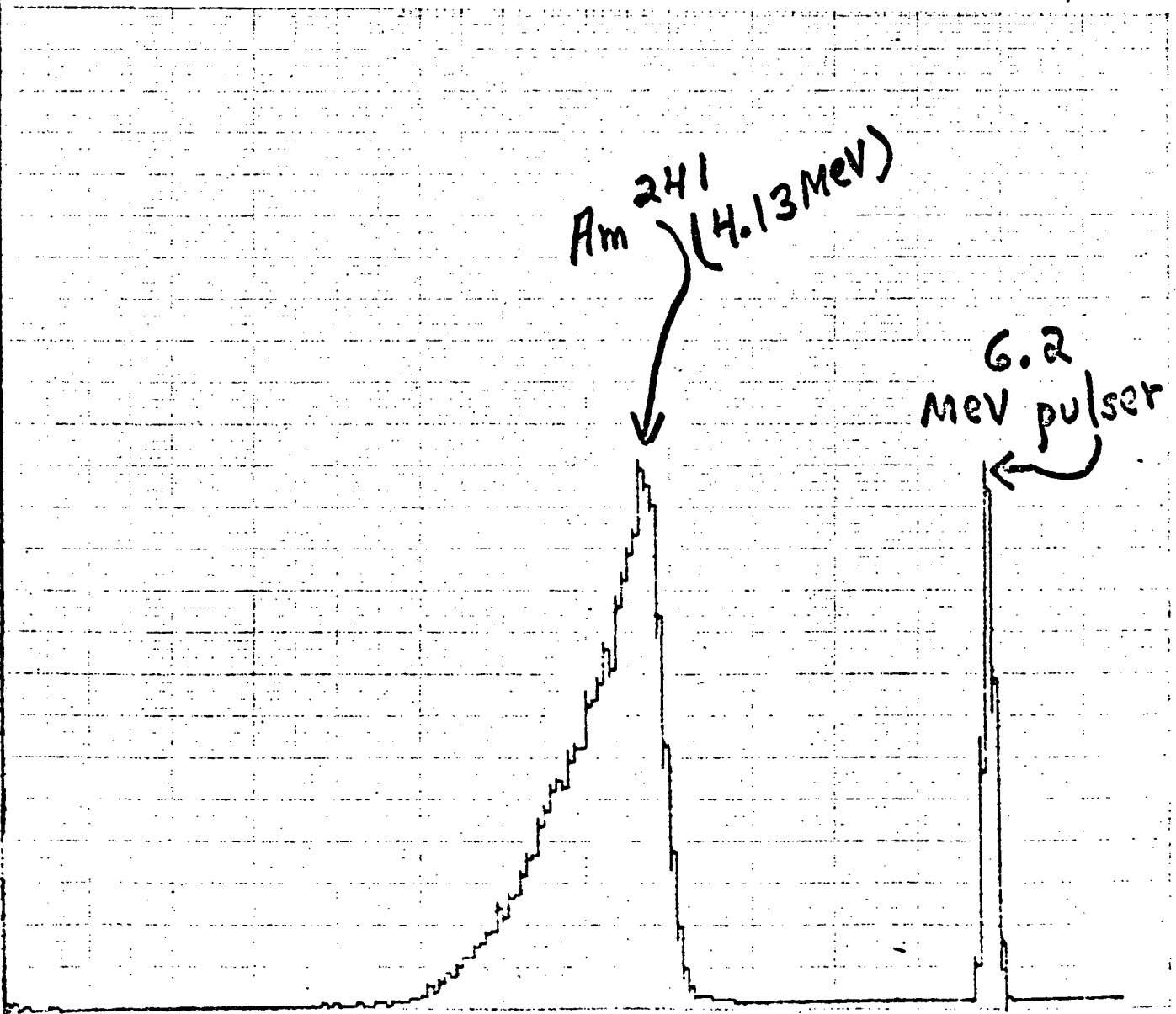




Det. #	L-1152		
Date:	12/19/71	Time	
Run #		Spec. #	
v	40 volts	I	7.0 $\mu$ A
Press.	F. pump	Temp.	Room $^{\circ}$ C
Pulser	6.2 MeV	Source	$Am^{241}$
$\Delta t$	1.0'	Amp. Const.	1 $\mu$ S
F.W.H.M.		C.C.E.	
Stored in		Horz. Scale	

$Am^{241}$  spectrum taken after exposure to  $1.1 \times 10^9$  200 MeV protons ( $1.2 \times 10^8$  protons/cm $^2$ )

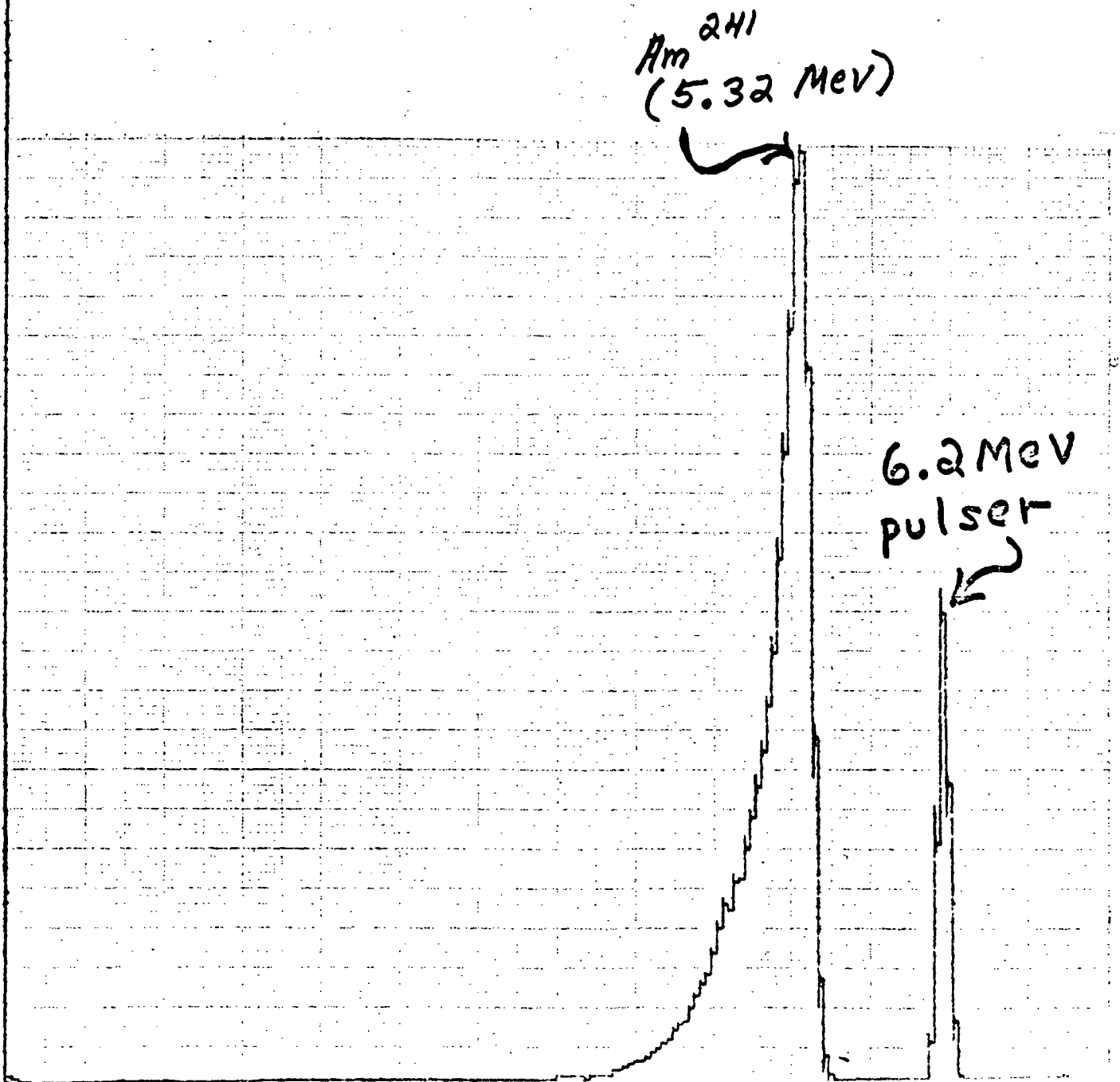
Figure 6.



Det. #	L-1152	
Date:	12/9/71	Time
Run #		Spec. #
V	80 Volts	7.5 $\mu$ A
Press.	F. Pump	Temp. Room $^{\circ}$ C
Pulser	6.2 MeV	Source $Am^{241}$
$\Delta t$	1.0'	Amp. Const. 145
F.W.H.M.		C.C.E.
Stored in		Horz. Scale

$Am^{241}$  spectrum taken after exposure to  $1.1 \times 10^9$  200 MeV protons. ( $1.2 \times 10^8$  protons/cm $^2$ )

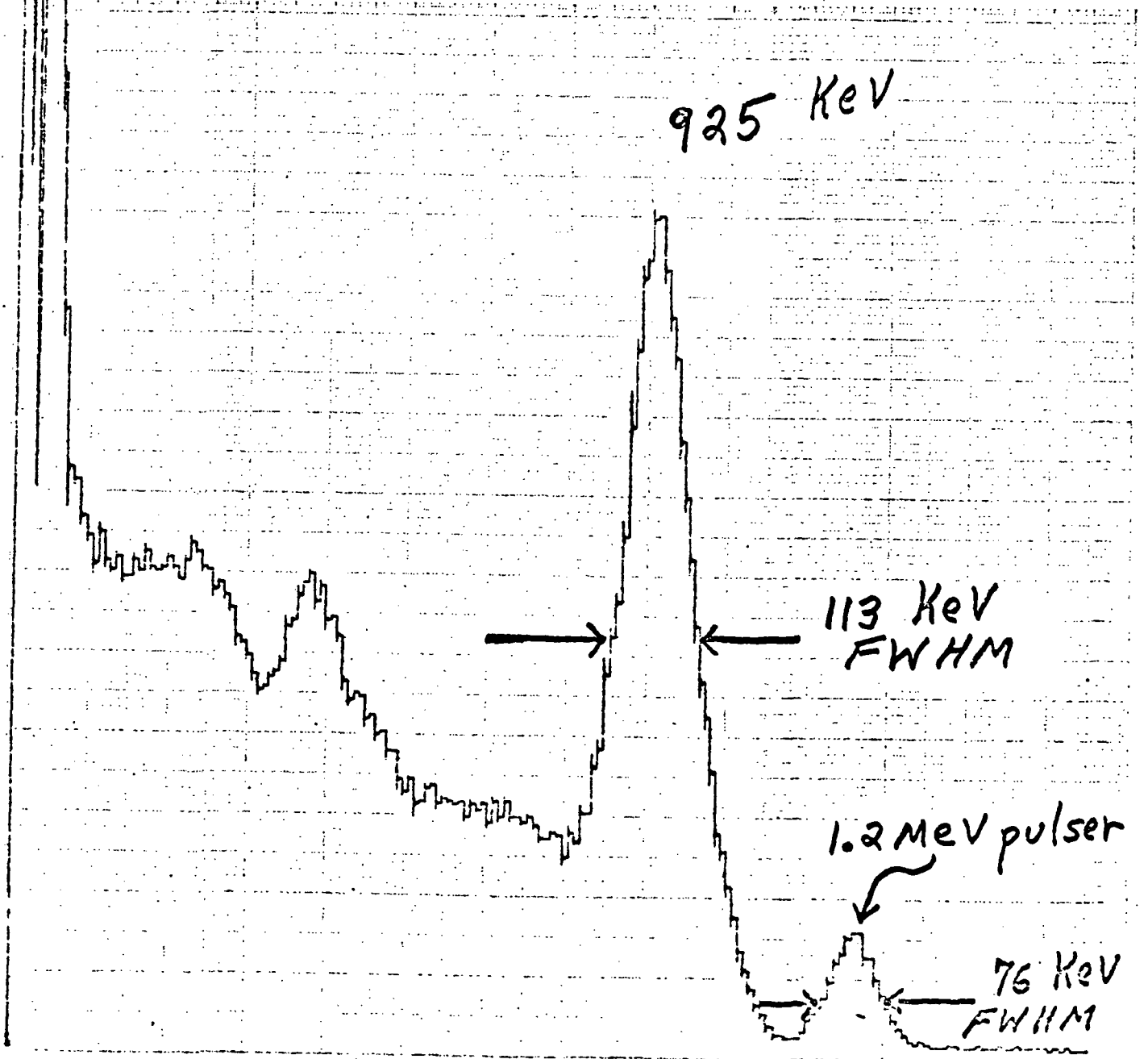
Figure 7.



Det. #	L-1152	
Date:	12/9/71	Time
Run #		Spec. #
V	40 Volts	6.5 $\mu$ A
Press.	ATM.	Temp. Room $^{\circ}$ C
Pulser	1.2 MeV	Source Bi <sup>207</sup>
$\Delta t$	1.0	Amp. Const. $1 \mu$ s
F.W.H.M.		C.C.E.
Stored in		Horz. Scale

Bi<sup>207</sup> spectrum taken  
 after exposure to  
 $1.1 \times 10^9$  200 MeV protons.  
 $(1.2 \times 10^8 \text{ protons/cm}^2)$

Figure 8.



## APPENDIX B

### I. Reports, memos, . etc., concerning RTG interference effects:

- 1) "RTG Tests with University of Chicago Pioneer-6 Telescope". (performed 1/17-19/66. D. R. Smith).
- 2) "Radiation Interference from a SNAP-27 Radioisotope Heat Source as observed by the University of Chicago Charged Particle Telescope For Pioneer F/G - Major Findings" (performed 10/20-24/69. J. J. O'Gallagher and S. Tejero).
- 3) "Report on Effect of RTG Radiation On The University of Chicago Instrument and Proposal to Recover Scientific Objectives of The Experiment" (J. A. Simpson and J. J. O'Gallagher, 11/17/69).
- 4) "Effectiveness of Heavy Metal Shielding Against  $\gamma$ -Rays from  $\text{Co}^{60}$  and  $\text{Na}^{24}$ ". (Performed 4/17-24/70. A. Tuzzolino and S. Tejero) -- Study of the Response of Lithium-drifted Silicon detectors to  $\text{Co}^{60}$  and  $\text{Na}^{24}$   $\gamma$ -rays as a function of shielding by various amounts of Tungsten, Uranium, Mallory 2000, and Platinum.
- 5) "Shielding Study for The University of Chicago Experiment on Pioneer F/G. (June 1970. C. Kelber and A. McArthy).
- 6) "New Values for Neutron Flux from Pioneer F RTG Fuel Capsules". (12/16/70. A. Tuzzolino). -- Study of the response of Lithium-drifted Silicon detectors to Neutrons.
- 7) "Summary of Effects of RTG Radiation on the University of Chicago Pioneer F/G Charged Particle Telescope Observed During the RTG/Spacecraft/Instrument Interference Test at TRW on April 4-6, 1971." (P. Walpole, S. Tejero, and A. Tuzzolino).
- 8) "Summary of Response of Pioneer F/G Main System Telescope to RTG Radiation Observed during the Second RTG/Spacecraft/Interference Test at TRW on December 16-18, 1971." (A. Tuzzolino, M. Perkins, and S. Tejero).
- 9) "Summary of results of  $\gamma$ -ray studies on L1 detectors and expected response of L1 detectors to MJS RTG radiation." (7/18/72. A. Tuzzolino).

### II. Reports, memos, etc. concerning intense fluxes of "trapped" particles,

i. e., radiation damage.

1) "Optical Coupling for Photomultipliers" (3/19/69. J. Jezewski) -- Studies of the effects of proton,  $\alpha$  -particle, and electron radiation on various optical coupling materials.

2) "Report on Radiation Damage Test Conducted at Hughes Aircraft, Fullerton, California." (2/26/70 to 3/17/70. W. Harvey and S. Tejero). -- Studies of the effects of  $\text{Co}^{60}$  radiation on: a) crystal clocks, b) T. I. low-power logic I. C. 's, c) Various NAND gates, d) various discrete components; e) AMI MOSFET devices; f) various operational amplifiers; g) various COSMOS circuits; h) various plastic scintillators; i) Corning glasses and various plastic materials; j) glass PM tube envelopes and various PM tube assemblies.

3) "Results of Argonne Van de Graaf Accelerator Run of 11/3-4/70". (B. McKibben and S. Tejero). -- Study of radiation damage in Lithium-drifted silicon detectors resulting from irradiation by electrons from 1-3 MeV.

4) "ECD Detector History". (9/11/70. B. McKibben). -- Study of radiation damage in Pioneer F/G ECD detectors resulting from irradiation by 1-3 Mev electrons.

5) "Summary of High-Energy Proton Damage Study of Lithium-Drifted Detectors of December 2-5, 1971, at SREL". (A. Tuzzolino).

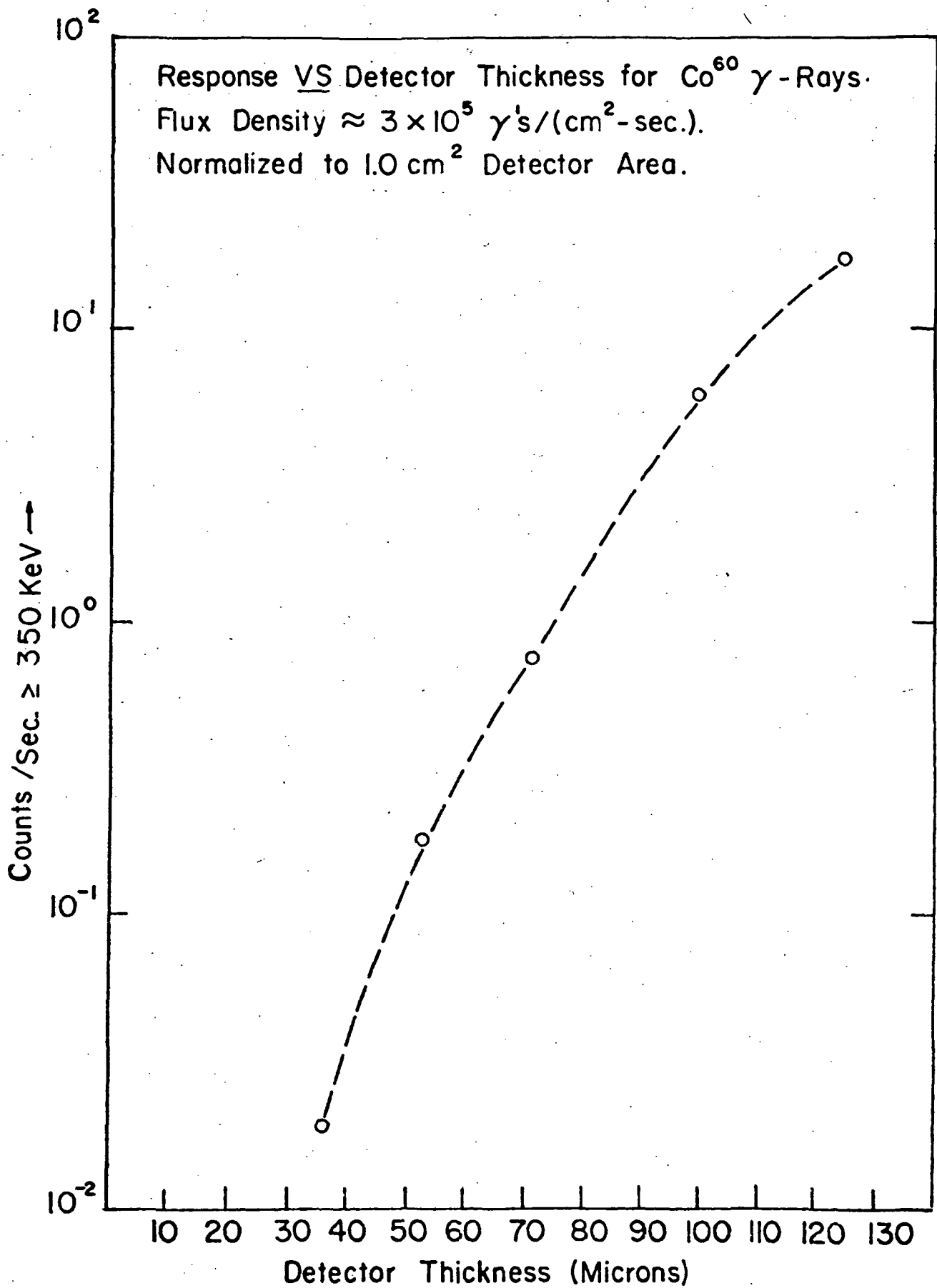


Figure 1

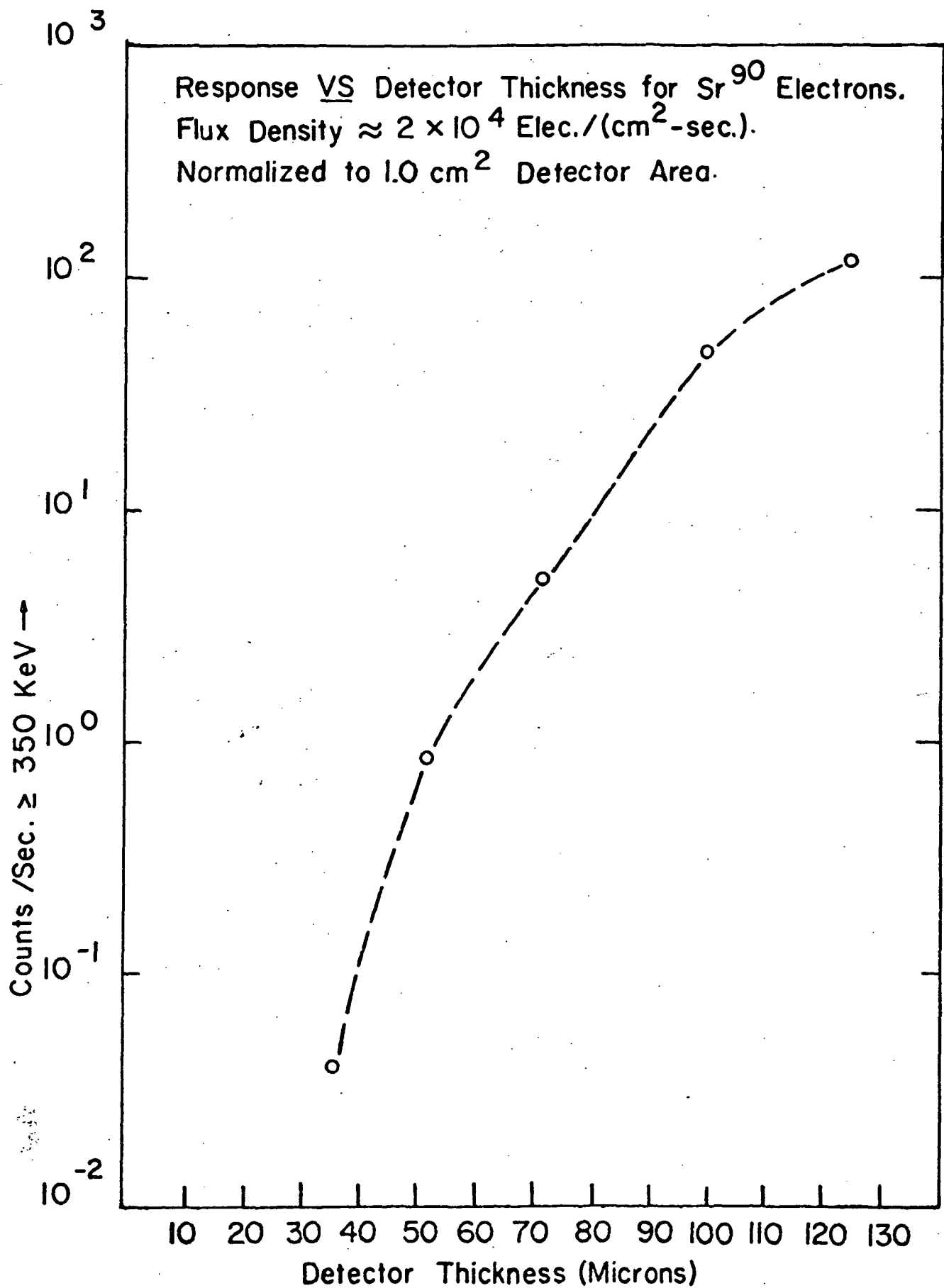
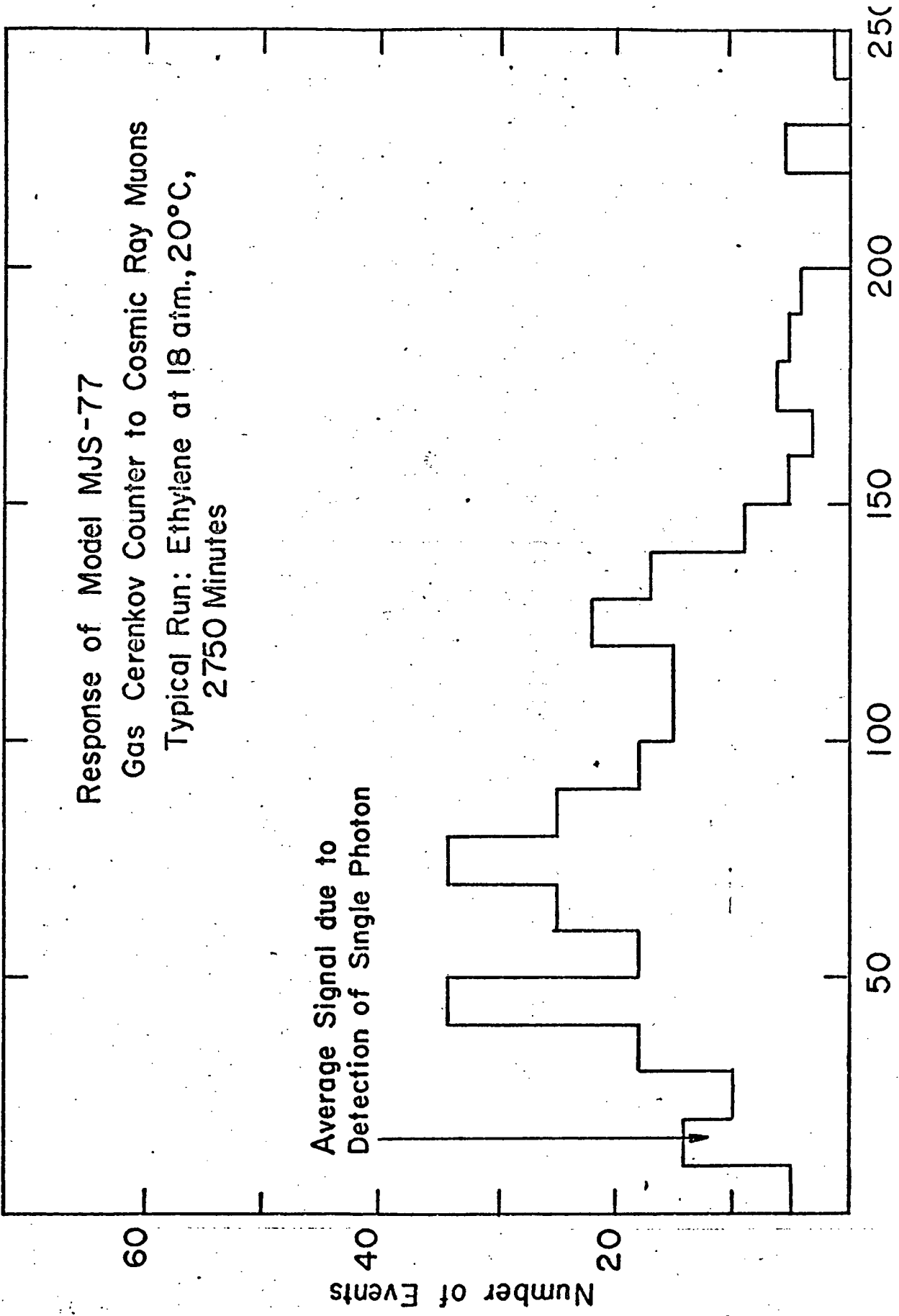


Figure 2

Response of Model MJS-77  
Gas Cerenkov Counter to Cosmic Ray Muons  
Typical Run: Ethylene at 18 atm., 20°C,  
2750 Minutes



Photomultiplier Output (arbitrary units)  
Figure 3

Response of MJS-77 Model Gas Cerenkov Counter to 195 MeV Protons

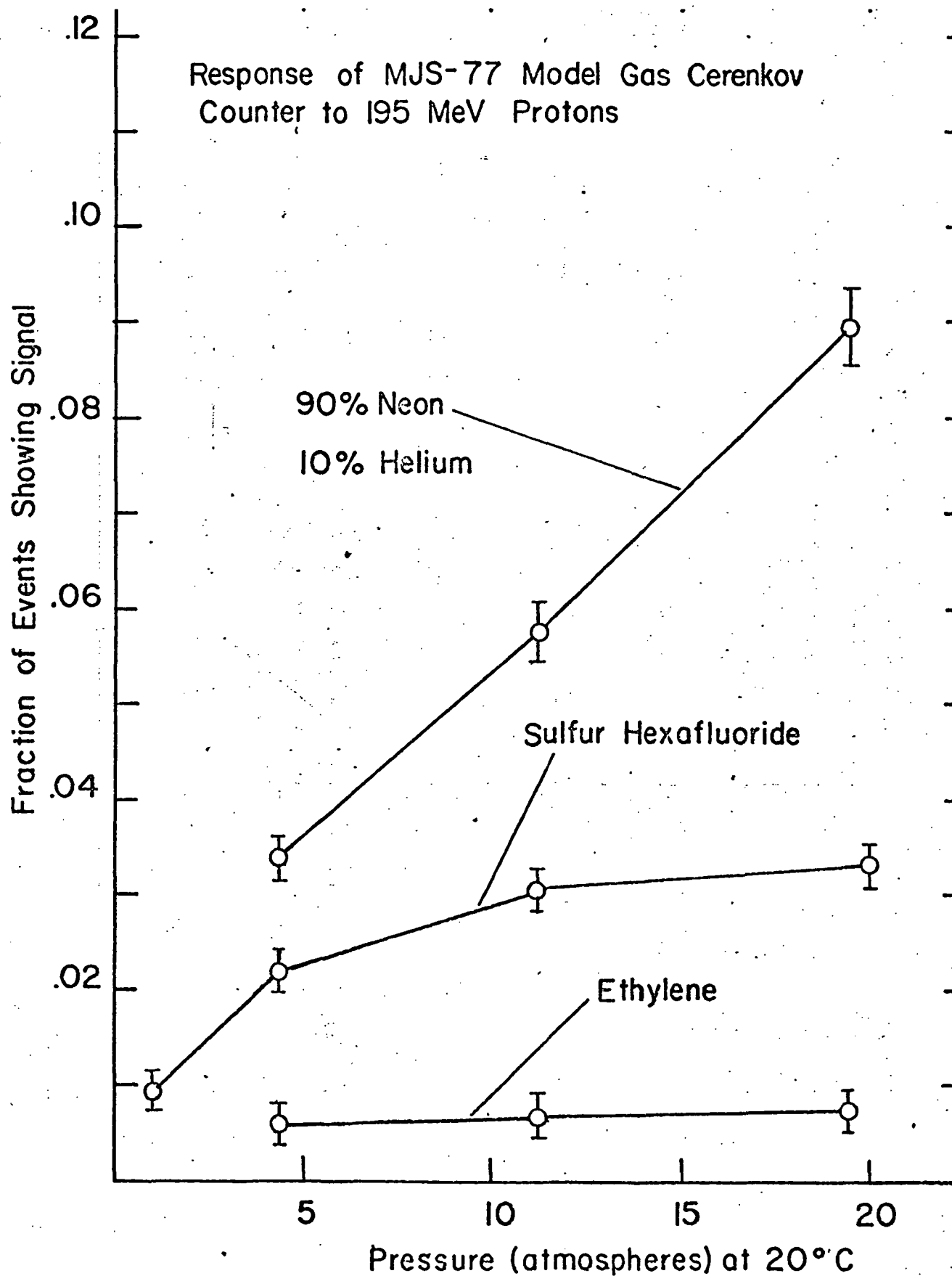
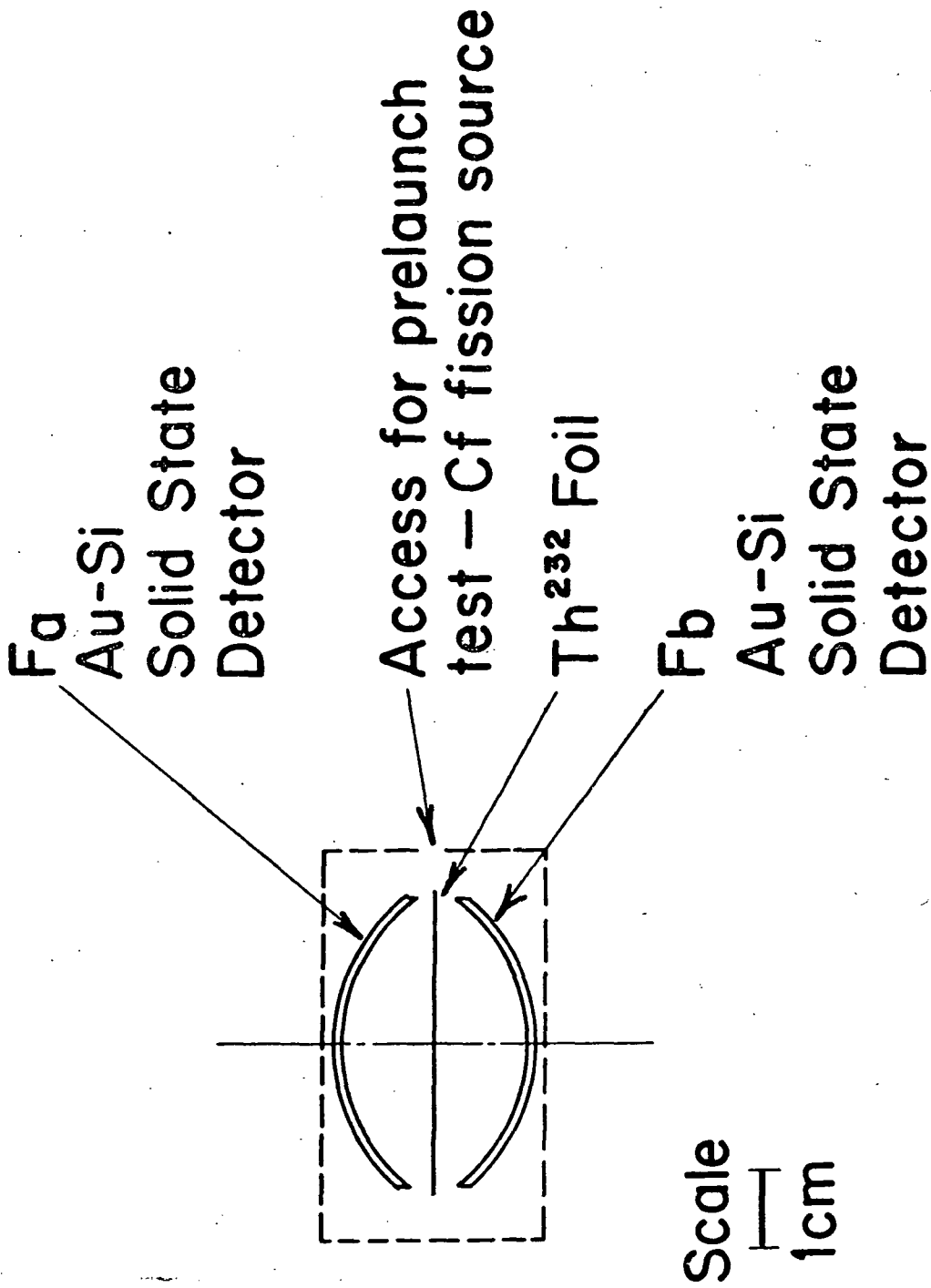


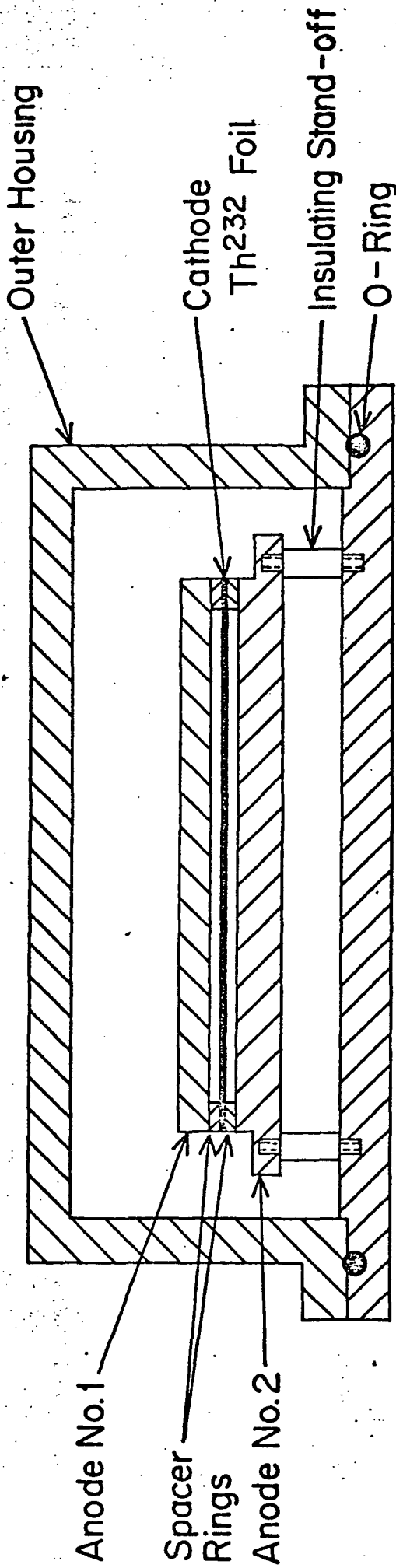
Figure 4



Proton Fission Cell  
 The University of Chicago

Figure 5

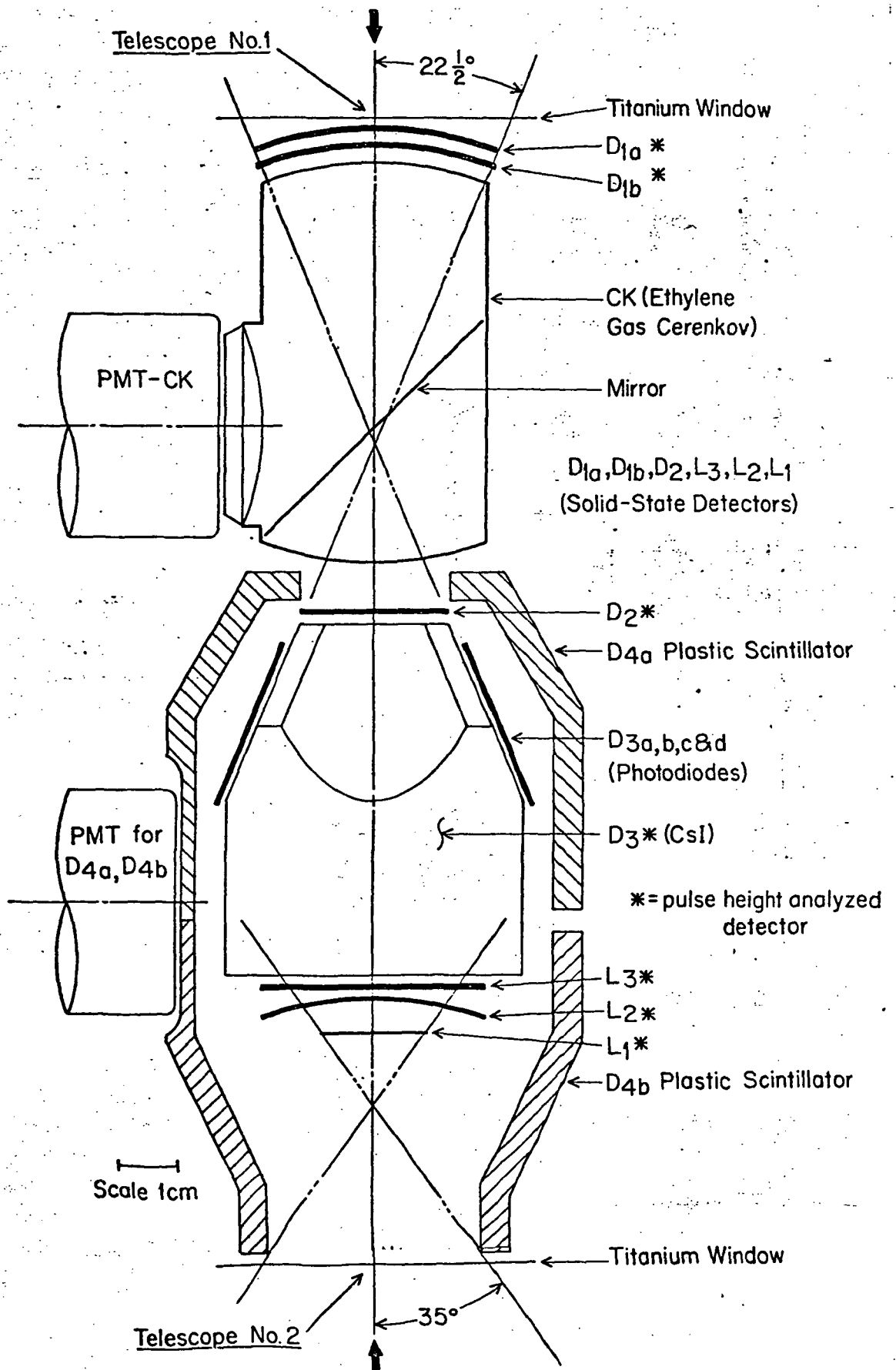
Not to Scale



Fission Ionization Chamber

The University of Chicago

Figure 6



Charged Particle Telescope for the  
 Mariner Jupiter-Saturn 1977 Mission  
 The University of Chicago  
 Figure 7

Incident Flux density (cm <sup>2</sup> -sec.) <sup>-1</sup>	W = 35.7μ					W = 52.2μ					W = 71.6μ					W = 100μ					W = 125μ							
	Pulses/sec. above:					Pulses/sec. above:					Pulses/sec. above:					Pulses/sec. above:					Pulses/sec. above:							
	350 KeV	400 KeV	450 KeV	500 KeV		350 KeV	400 KeV	450 KeV	500 KeV		350 KeV	400 KeV	450 KeV	500 KeV		350 KeV	400 KeV	450 KeV	500 KeV		350 KeV	400 KeV	450 KeV	500 KeV		350 KeV	400 KeV	450 KeV
Co <sup>60</sup> (γ-rays) 3.2x10 <sup>5</sup>	0.019	0.009	-	-	-	0.18	0.07	0.06	-	-	0.76	0.28	0.11	0.04	-	6.1	2.6	1.2	0.37	-	17.1	8.5	4.2	1.8	-	-	-	-
Bi <sup>207</sup> (electrons) 1x10 <sup>3</sup>	0.007	0.003	-	-	-	0.09	0.07	0.04	-	-	0.26	0.09	0.02	-	3.3	1.7	0.84	0.31	-	7.7	4.3	2.4	1.0	-	-	-	-	
Sr <sup>90</sup> (electrons) 2x10 <sup>4</sup>	0.04	0.01	-	-	-	0.88	0.22	0.07	0.05	-	5.1	1.83	0.54	0.20	-	18.4	34.4	12.8	5.5	-	119	67	37	18	-	-	-	-
Cs <sup>137</sup> (electrons) 1x10 <sup>4</sup>	0.002	-	-	-	-	0.11	0.05	0.04	-	-	0.32	0.10	0.03	0.02	-	2.8	1.0	0.27	0.07	-	6.9	2.6	0.8	0.2	-	-	-	-

TABLE 1

Response of silicon detectors to γ-rays and electrons  
as a function of discriminator level and detector  
thickness. All values are normalized to a detector  
area of 1.0 cm<sup>2</sup>.

TABLE 2: Energy Ranges and Particle Identification

TELESCOPE NO. 1

(Energy in MeV/nucleon for Nuclear Particles Incident at 0°)

Particle	Range Coin- cidence	CK Not Triggered		CK Triggered		
		D1D2D3L3	D1D2D3L3	D1D2D3	D1D2D3L3	D1D2D3L3
e		-	-	5 - 15	15 - 200	200 - ~ 500
H		39 - 150	> 150	See Note 1		> 5000
He		39 - 150	> 150	"		> 5000
O		82 - 340	> 340	"		≥ 5000
Si		112 - 480	> 480	"		≥ 5000
Fe		150 - 700	> 700	"		≥ 5000

Note 1: Nucleons triggering the CK always pass through the telescope and fire L3.

TELESCOPE NO. 2

Particle	Range Coin- cidence	L1L2	L1L2L3	L1L2L3D3	L1L2L3D3D2
		Immune at all energies - - - - -			
H		0.5 - 2.6	2.6 - 11.5	11.5 - 20.5	20.5 - 150
He		0.3 - 2.6	2.6 - 11.5	11.5 - 20.5	20.5 - 150
O		0.8 - 6.1	6.1 - 26.5	26.5 - 36	36 - 340
Si		1.1 - 8.3	8.3 - 35	35.0 - 51	51 - 480
Fe		1.6 - 11.0	11.0 - 49	49 - 68	68 - 700

Geometrical Factors for Telescope

Telescope No. 1 (	D1 <sub>a</sub> D2D3D4	=	0.67 cm <sup>2</sup> -sr	} Trajectories E, F
(	D1 <sub>b</sub> D2D3D4	=	0.74 cm <sup>2</sup> -sr	
Telescope No. 2	L1L2D4	=	1.41 cm <sup>2</sup> -sr	Trajectories A,B,C,D